Cellular and Molecular Life Sciences (2025) 82:219
https://doi.org/10.1007/s00018-025-05751-4

ORIGINAL ARTICLE

GPR35 prevents drug-induced liver injury via the Gαs-cAMP-PKA axis in macrophages

Xueqin Zhao[1] · Yuanhao Li[1] · Liu Yang[1] · Xi Chen[1] · Jialong Zhang[1] · Tong Chen[2] · Haoqi Wang[1] · Fei Li[1] · Chen Cheng[1] · Jingjing Wu[3] · Jingjing Cong[1] · Wenwei Yin[4] · Jing Li[2] · Xuefu Wang[1]

Received: 10 December 2024 / Revised: 31 March 2025 / Accepted: 13 May 2025

Abstract

Acetaminophen (APAP) overdose induces acute liver injury and represents the most frequent cause of drug-induced liver injury worldwide. Macrophage-mediated inflammation plays detrimental roles during the early stage of liver injury. However, the potential targets regulating inflammation to improve drug-induced liver injury remains undefined. In this study, we reported that G protein-coupled receptor 35 (GPR35) improves drug-induced liver injury by blocking macrophage-mediated inflammation via the Gαs-cyclic AMP-protein kinase A (Gαs-cAMP-PKA) pathway. The ablation of GPR35 exacerbates APAP-induced liver injury, characterized by higher levels of alanine aminotransferase and aspartate aminotransferase in sera, larger damaged areas, and increased levels of pro-inflammatory cytokines. More hepatic macrophages appeared in the inflamed liver of mice with GPR35 deficiency. In contrast, the agonists of GPR35 alleviated APAP-induced liver injury. The depletion of macrophages abolished GPR35-mediated protection. Mechanistically, GPR35 ablation facilitated the activation of pro-inflammatory AKT, MAPK, and NF-κB signaling pathways at the downstream of Toll-like receptors in macrophages. GPR35 agonists activated Gαs-cAMP-PKA signaling to inhibit the activation of these pro-inflammatory signaling pathways and then suppress the inflammatory response in macrophages. Thus, our findings demonstrate that GPR35 prevents drug-induced liver injury by blocking macrophage-mediated inflammation via the Gαs-cAMP-PKA pathway, indicating that GPR35 is a potential target for the development of novel medicines that control drug-induced liver injury.

Keywords G protein-coupled receptor 35 · Macrophages · CAMP · Acetaminophen · Drug-induced liver injury

Introduction

Acetaminophen (APAP) is a widely-used analgesic and antipyretic drug, which is safe at therapeutic doses. Nevertheless, APAP overdose leads to acute liver injury and failure, and is becoming a major cause of drug-induced liver damage worldwide [1]. Mechanistically, an overdose of APAP generates an excess of N-acetyl-p-benzoquinone imine (NAPQI), which consumes hepatic glutathione (GSH), and subsequently leads to hepatocyte death [2]. Moreover, The following inflammatory response, characterized by the release of damage-associated molecular pattern molecules from dead hepatocytes, further aggravates liver injury and eventually causes liver failure in a second-hit manner [3]. The unsatisfactory efficacy of treatment with N-acetyl-L-cysteine to improve NAPQI-induced oxidative damage results from the narrow therapeutic window, indicating that the inflammatory process may be a more feasible target for

✉ Wenwei Yin
yww@cqmu.edu.cn

✉ Jing Li
lijing1812@ahmu.edu.cn

✉ Xuefu Wang
wangxuefu@ahmu.edu.cn

1 School of Pharmacy, Inflammation and Immune Mediated Diseases Laboratory of Anhui Province, Anhui Medical University, #81 Meishan Road, Hefei 230032, Anhui, China

2 School of Life Sciences, Anhui Medical University, #81 Meishan Road, Hefei 230032, Anhui, China

3 Department of Oncology, The Second Affiliated Hospital of Anhui Medical University, Hefei 230601, China

4 Institute for Viral Hepatitis, Department of Infectious Diseases, The Second Affiliated Hospital, Chongqing Medical University, Chongqing 400016, China

Published online: 29 May 2025

intervention [4, 5]. Diverse immune cells have been shown to play detrimental roles in APAP-induced liver injury [6]. Our previous study demonstrated that hepatic macrophages act as the central controller of hepatic inflammatory damage following an overdose of APAP [7]. Hepatic macrophages aggravate APAP-induced hepatotoxicity at the early stage of the damage process [8]. The depletion of hepatic macrophages through pre-treatment with liposomal clodronate protects against APAP-induced hepatotoxicity [9]. Preventing the liver recruitment of monocyte-derived macrophages also mitigates APAP-induced hepatotoxicity [10]. Additionally, inhibiting of NF-κB signaling in hepatic macrophages attenuates APAP-induced hepatotoxicity [11]. Therefore, identifying druggable targets that prevent liver infiltration by macrophages and inhibit their inflammatory response is crucial for improving APAP-induced hepatotoxicity.

G protein-coupled receptors (GPCRs) are the largest family of membrane receptors. They mediate diverse types of diseases, such as hypertension, sepsis, and cancer. Therefore, they have become targets of approximately 30–40% of marketed drugs [12]. GPCRs couple with heterotrimeric G proteins composed of Gα, Gβ, and Gγ subunits, which bind to downstream effectors upon GPCR activation, and generate second messengers, such as Ca^{2+}, cyclic AMP (cAMP), and inositol phosphates [13]. G protein-coupled receptor 35 (GPR35) belongs to the orphan GPCR family, and is highly expressed on immune cells and in gastrointestinal tissues [14]. GPR35 can be activated by endogenous ligands, including lysophosphatidic acid (LPA), pamoic acid (PA), kynurenic acid (KA), and 5-hydroxyindoleacetic acid (5-HIAA), as well as synthetic molecules, such as disodium cromoglycate (DSCG) and zaprinast [15–19]. Accumulating studies have demonstrated that GPR35 is involved in multiple diseases, including hypertension, heart failure, pain, metabolic syndrome, and inflammatory bowel disease [20–22]. Our group has revealed that GPR35 defends against NLRP3-mediated inflammatory diseases and attenuates nonalcoholic steatohepatitis [23, 24]. However, the role of GPR35 in APAP-induced liver injury remain poorly understood.

In the present study, we demonstrated that GPR35 deficiency exacerbates APAP-induced liver injury. GPR35 alleviates inflammatory response in hepatic macrophages to improve APAP-induced liver injury via the Gαs-cAMP-PKA pathway. Thus, GPR35 plays a protective role in drug-induced liver injury and acts a potential target to prevent drug-induced liver failure.

Materials and methods

Mice

Wild type (WT) male and female C57BL/6 J mice (age: 6–8 weeks) were purchased from Shanghai SLAC Laboratory Animal Co., Ltd (Shanghai, China). *Gpr35*$^{-/-}$ mice (C57BL/6 J background) were purchased from Bioraylab Company (Shanghai, China). All mice were housed in a specific pathogen-free, temperature-controlled environment with unrestricted access to food and water at the animal facilities of the University of Science and Technology of China (Hefei, China). The environment was maintained at 22.5 °C, 42.5% humidity, and a 12-hour light-dark cycle. All experiments were performed according to the Guide for the Care and Use of Laboratory Animals of the University of Science and Technology of China and Anhui Medical University (Hefei, China). The study was approved by the Local Ethics Committee for Animal Care and Use at Anhui Medical University.

Treatment of mice

APAP (Yuanye Company, Shanghai, China) was dissolved in PBS at 40 °C. Mice were randomly assigned to received either PBS or APAP (300 or 400 mg/kg) via intraperitoneal injection after fasting for 16 h. Liver and blood samples were collected at specified time points following APAP administration. For lipopolysaccharide/D-galactosamine (LPS/D-GalN)-induced liver injury, mice were administered D-GalN (intraperitoneal injection, 500 mg/kg; Yuanye Company, Shanghai, China) and LPS (intravenous injection, 50 μg/kg; *E. Coli* O111:B4, Sigma-Aldrich). Mice were scarified 6 h after LPS/D-GalN administration. To deplete hepatic macrophages, mice were treated with either $GdCl_3$ (10 mg/kg, Sigma-aldrich, USA) or clodronate/liposome (200 μl/mouse, Vrije Universiteit Amsterdam, Yeasen, USA) via intravenous injection 24 and 72 h prior to APAP administration, respectively. To determine the effects of KA and DSCG on APAP- or LPS/D-GalN-induced liver injury, mice were treated with either KA (500 mg/kg; Aladdin, Shanghai, China) or DSCG (500 mg/kg; Aladdin, Shanghai, China) prior to APAP administration.

GSH measurement

Fresh liver tissues were homogenized, and protein concentration was subsequently measured. The hepatic concentration of GSH was measured using a Total GSH Quantification kit (Solarbio Life Science, Beijing, China) and determined by spectrophotometry according to the manufacturer's

instructions. GSH concentration were normalized to the amount of fresh liver tissue (nmol/mg liver tissue).

Assessment of liver injury

Liver injury was assessed based on serum levels of alanine aminotransferase (ALT) and aspartate aminotransferase (AST), as well as histological analyses. ALT and AST levels were quantified using a diagnostic kit (Mindray Bio, Shenzhen, China). Liver specimens were fixed in 4% paraformaldehyde, dehydrated, and embedded in paraffin. Liver sections were prepared and stained with hematoxylin and eosin for histochemical evaluation.

Measurement of cytokines using ELISA

Sera, organ homogenates, and cell culture supernatants were prepared for the measurement of cytokines. The amounts of TNF-α, IL-1β, IL-1α, monocyte chemoattractant protein-1 (MCP-1), IL-6, IL-4, and IL-10 were measured using commercially available ELISA Kits (Dakewei, Shanghai, China) according to the instructions provided by the manufacturer.

Analysis of cytokines through quantitative reverse-transcription polymerase chain reaction (qRT-PCR)

Total RNA was isolated from liver tissues or purified macrophages using total RNA purification reagents (Invitrogen, Thermo Fisher Scientific, CA, USA). RNA (2 μg) was reverse-transcribed using RT kits (Invitrogen, Thermo Fisher Scientific, CA, USA). Complementary DNA was amplified to measure the messenger RNA (mRNA) expression of TNF-α, IL-1β, IL-1α, MCP-1, IL-6, IL-4, and IL-10 using commercially available SYBR Premix Ex Taq (TaKaRa Biotechnology, Dalian, China) and specific primers (Supporting Table 1) in a reaction with 35 cycles at 95 °C for 10 s and at 60 °C for 30 s in a CFX Connect™ real-time PCR system (BIO-RAD, CA, USA). Gene expression levels were normalized to those of the housekeeping gene glyceraldehyde-3-phosphate dehydrogenase (GAPDH).

Isolation of hepatic lymphocytes and flow cytometry analysis

Mouse liver tissue was harvested, pressed through a 200-gauge stainless steel mesh, suspended in PBS, and centrifuged at 50 × *g* for 1 min. Supernatants were transferred into fresh tubes and centrifuged again at 800 × *g* for 10 min. Pellets were resuspended in 40% Percoll® (GE Healthcare, MA, USA), layered onto 70% Percoll®, and centrifuged at 1,260 × *g* for 30 min at room temperature. The intermediated layer cells were collected, washed with PBS, and counted using a cell counter (Celldrop; DeNovix Inc., DE, USA). Cells (1×10^6) were stained with FITC-anti mouse CD45.2, PE-anti mouse CD4, PerCP-Cy5.5-anti mouse CD8, APC-Cy7-anti mouse CD3, and PE-Cy7-anti mouse NK1.1. Testing was performed on a CytoFLEX flow cytometer (Beckman, CA, USA), and the results were analyzed using the Flowjo software (Treestar, Ashland, OR, USA).

Isolation, flow cytometry analysis, and sorting of hepatic macrophages

Hepatic macrophages were isolated from mice using a liver perfusion collagenase system as previously reported [25]. Briefly, the liver was perfused with ethylene glycol tetraacetic acid for 5 min, followed by IV-type collagenase for 10 min, chopped, and filtered through a 70-μm strainer. The non-parenchymal cell fraction was acquired after centrifugation at 50 × *g* for 5 min. The supernatant was centrifuged at 500 × *g* for 10 min. The pellets were resuspended in 20% Percoll® (GE Healthcare), carefully layered onto 50% Percoll®, and centrifuged at 800 × *g* for 30 min. The hepatic macrophage fraction was collected from the intermediated layer between the two Percoll® gradient layers. Cells were counted and used for flow cytometry analysis or cell sorting. For flow cytometry analysis, cells were stained with FITC-anti-mouse CD11b, PE-CY7-anti-mouse CD45.2, APC-anti-mouse F4/80, APC-CY7-anti-mouse Ly6G. For cell sorting, cells were stained with PE-F4/80 and incubated with anti-PE beads (130-048-801; Miltenyi Biotech, Germany). The purified hepatic macrophages (purity >90%) were used for RNA sequencing to determine the mRNA levels of cytokines using qRT-PCR or protein levels of genes of interest by western blotting.

RNA sequencing analysis

RNA sequencing (RNA-seq) was performed on total RNA isolated from hepatic macrophages of WT and *Gpr35*$^{-/-}$ mice at 12 h after APAP treatment, with triplicate samples. Sequencing libraries were generated using the TruSeq RNA Sample Preparation kit (Illumina). RNA-seq analysis was conducted by OE Biotech Co., Ltd (Shanghai, China).

Preparation and treatment of peritoneal macrophages

Peritoneal macrophages were prepared and harvested as previously described [26]. Briefly, mice were injected intraperitoneally with 1 ml of 3% Brewer thioglycollate broth (BBL™ Thioglycollate Medium Brewer Modified; BD Biosciences, MD, USA). At 72 h post-injection, peritoneal exudate cells were collected in cold PBS and centrifuged

at 400 × *g* for 10 min. The cell pellet was resuspended in cold DMEM, and the cells were counted. Cells (2×10^6) were plated in six-well plates and cultured for 2 h at 37 °C. Non-adherent cells were subsequently removed using warm PBS. The adherent peritoneal macrophages in were used for subsequent experiments. For activation of inflammatory signaling, peritoneal macrophages were stimulated with LPS (0.3 μg/ml) for 1 h for the protein assay, or LPS (1 μg/ml) for 18 h for cytokine production. The GPR35 agonist KA (4 mM), DSCG (200 μg/ml), 5-HIAA (10 μm, MedChemExpress, NJ, USA) and Zaprinast (10 μm, MedChemExpress, NJ, USA) was administered 1 h before LPS treatment. Adenylate cyclase (AC) activator forskolin (FSK; 10 μM, MedChemExpress, NJ, USA) was used to stimulate cAMP in peritoneal macrophages 1 h prior to LPS treatment. To investigate the role of Gαs-cyclic AMP-protein kinase A (Gαs-cAMP-PKA) in the GPR35-mediated effect on macrophages, the Gαs inhibitor NF449 (25 μM, Santa Cruz Biotechnology, TEX, USA), AC inhibitor SQ22536 (50 μM, MedChemExpress, NJ, USA), or PKA inhibitor H89 (10 μM, MedChemExpress, NJ, USA), PKA inhibitor fragment [6–22] amide (10 μm, TargetMol, BOS, USA) was added to the culture 30 min prior to treatment with the GPR35 agonist.

Western blotting and co-immunoprecipitation (Co-IP)

Macrophages exposed to different treatments were harvested and lysed in radioimmunoprecipitation assay buffer (Beyotime, Shanghai, China) supplemented with protease inhibitors and phosphatase inhibitors (Beyotime, Shanghai, China). Cell debris was removed by centrifugation at 12,000 × *g* for 5 min. The protein concentration was subsequently determined using bicinchoninic acid assay (Beyotime, Shanghai, China) according to the manufacturer's instructions. Equal amounts of protein were separated by 10% SDS-PAGE and transferred to polyvinylidene difluoride (PVDF) membranes. The membranes were incubated overnight at 4 °C with primary antibodies against proteins of interest (Anti-GPR35 [1:1000; NBP2-24640; Novus, CO, USA], Anti-CYP2E1 [1:1000; NBP1-85367; Novus, CO, USA], Anti-p-AKT [1:1000; #9271; Cell Signaling, MA, USA], Anti-Bcl2 [1:1500; 26593-1-AP; Proteintech; Wuhan, China], Anti-Bax [1:5000; 50599-2-Ig; Proteintech; Wuhan, China], Anti-AKT [1:1000; #9272; Cell Signaling, MA, USA], Anti-p-p38 [1:1000; #4511; Cell Signaling, MA, USA], Anti-p38 [1:1000; #9212; Cell Signaling, MA, USA], Anti-p-p65 [1:1000; #3033; Cell Signaling, MA, USA], Anti-p65 [1:1000; #8242; Cell Signaling, MA, USA], Anti- Phospho-PKA C (Thr197) [1:1000; #5661; Cell Signaling, MA, USA] and Anti-β-actin [1:10000; ab8227; Abcam, CA, USA], Anti-GNAS [1:1000; Proteintech; 10150-2-AP; Wuhan, China]; Anti-GNA13 [1:1000; 67188-1-Ig; Proteintech; Wuhan, China]). Membranes were then incubated with horseradish peroxidase-conjugated secondary antibodies (1:5000) for 1 h at room temperature and detection was performed by chemiluminescence autoradiography. Co-immunoprecipitation (Co-IP) was performed to assess the interaction between GPR35 and Gαs. Peritoneal macrophages were stimulated with KA for 30 min, lysed in radioimmunoprecipitation assay buffer, and incubated with anti-GPR35 antibody (Novus, CO, USA). The protein complex was subsequently captured using Protein A/G agarose and precipitated. Western blotting was used to detect Gαs using an anti-Gαs antibody (1:1000; Santa Cruz Biotechnology, Santa Cruz, CA, USA).

cAMP assay

Cyclic AMP (cAMP) production was measured using the LANCE®Ultra cAMP (PerkinElmer, PA, USA). Briefly, 1×10^6 macrophages were stimulated with GPR35 agonists or the AC activator FSK for 30 min at 37 °C. Macrophages (5×10^3 per well) were seeded in a 384-well plate, treated with test compounds for the indicated time before lysis, and analyzed using a luminometer (SpectraMax iD5; Molecular Devices, San Jose, CA, USA) according to the manufacturer's instructions.

Statistical analysis

GraphPad Prism 9.0 (La Jolla, CA) was used for all statistical analyses. Statistical analysis was applied to biological replicates, or biologically independent mice for each experiment. All experiments described in this study have been performed at least three times. Data are presented as the mean ± SEM. Two-tailed Student's t test was used to determine statistical significance between two groups and two-way ANOVA was used when data were compared based on multiple curves. P-values < 0.05 denoted statistically significant differences. Significance levels were denoted by *, **, and ***, representing p-values of < 0.05, < 0.01, and < 0.001. respectively. Figure illustrations in the article were created using BioRender software. Specifics regarding sample sizes, measures of dispersion, and the statistical tests used can be found in the figure legends.

Results

GPR35 ablation aggravates APAP-induced liver injury

To investigate the role of GPR35 in APAP-induced liver injury, male wild type (WT) and *Gpr35*$^{-/-}$ mice were fasted overnight and treated with 400 mg/kg of APAP. The levels of alanine aminotransferase (ALT) and aspartate aminotransferase (AST) in *Gpr35*$^{-/-}$ mice at 12 h after treatment with APAP were significantly higher than those measured in male WT mice (Fig. 1A). Histopathological examination displayed more pronounced centrilobular necrosis and massive hepatocyte death in male *Gpr35*$^{-/-}$ mice compared with male WT mice (Fig. 1B). Similar findings were observed in female WT and *Gpr35*$^{-/-}$ mice (Fig. 1C and D), suggesting that *Gpr35*$^{-/-}$ mice are more susceptible to APAP-induced liver injury. Moreover, 400 mg/kg of APAP led to a high lethality of *Gpr35*$^{-/-}$ mice at 12 h after treatment. Therefore, to further confirm these results, WT and *Gpr35*$^{-/-}$ mice were treated with 300 mg/kg of APAP and analyzed at 24 h after treatment. Consistently, *Gpr35*$^{-/-}$ mice developed more severe liver injury, characterized by higher levels of ALT and AST in serum at 24 h after treatment with APAP, compared with WT mice (Fig. 1E and F). Next, we examined the apoptotic effects at this time point and observed a significant increase in pro-apoptotic Bax levels along with the suppression of anti-apoptotic Bcl-2 in *Gpr35*$^{-/-}$ mice (Supporting Fig. 1). Furthermore, during the liver repair phase at 48- and 72-hours post-APAP administration, serum ALT and AST levels remained higher in *Gpr35*$^{-/-}$ mice compared to WT mice, indicating impaired liver recovery in the absence of GPR35 (Fig. 1G and H). Taken together, these findings demonstrated that GPR35 protects against APAP-induced liver injury and plays a crucial role in liver repair.

GPR35 ablation aggravates APAP-induced liver injury via hepatic macrophages

We previously identified that hepatic immune cells mediate APAP-induced liver injury in our previous study [7]. To identify the changes of immune cells in the absence of GPR35, we analyzed hepatic immune cells in WT and *Gpr35*$^{-/-}$ mice after treatment with APAP. There was no significant difference in the frequency of hepatic natural killer (NK) cells, eosinophils, dendritic cells (DCs), natural killer T (NKT) cells, CD4^{+} T cells, and CD8^{+} T cells between WT and *Gpr35*$^{-/-}$mice. But *Gpr35*$^{-/-}$mice exhibited a reduction in hepatic neutrophils (Supporting Fig. 2). More importantly, there were more F4/80^{+} macrophages and CD11b^{high}F4/80^{int} infiltrating monocyte-derived macrophages (MoMFs) in *Gpr35*$^{-/-}$ mice versus WT mice, as shown by the higher frequency and the greater absolute number of F4/80^{+} macrophages and MoMFs in the liver (Fig. 2A and B). In contrast, the frequency of CD11b^{int}F4/80^{high} Kupffer cells was reduced in the liver of *Gpr35*$^{-/-}$ mice (Fig. 2B, Supporting Fig. 3). Accompanied by more MoMFs, the levels of pro-inflammatory cytokines IL-1α, IL-1β, MCP-1, and TNF-α were higher in the serum and liver of *Gpr35*$^{-/-}$ mice (Fig. 2C, D and E). Moreover, hepatic macrophages from *Gpr35*$^{-/-}$ mice displayed higher levels of pro-inflammatory cytokines compared to those obtained from WT mice (Fig. 2F). To confirm the role of hepatic macrophages in GPR35-mediated liver protection, we depleted hepatic macrophages using $GdCl_3$. The depletion of hepatic macrophages diminished APAP-induced liver injury both in WT and *Gpr35*$^{-/-}$ mice. Of note, the difference in APAP-induced liver injury between *Gpr35*$^{-/-}$ mice and WT mice disappeared; the animals showed similar levels of ALT and AST, and damaged areas (Fig. 3A and B). The difference in pro-inflammatory cytokines in the serum was also eliminated after the depletion of hepatic macrophages (Fig. 3C). The depletion of hepatic macrophages by clodronate/liposomes at 3 h after treatment with APAP also attenuated APAP-induced liver injury, as demonstrated by the reduced levels of ALT (Fig. 3D). Collectively, our findings demonstrate that GPR35 protects against APAP-induced liver injury by regulating hepatic macrophages.

GPR35 suppresses the inflammatory response in hepatic macrophages

To investigate the underlying mechanisms by which GPR35 suppressed inflammation in hepatic macrophages, we performed RNA sequencing (RNA-seq) on sorted F4/80^{+} hepatic macrophages from APAP-treated *Gpr35*$^{-/-}$ and WT mice. Differential gene expression analysis identified 871 genes were differentially expressed (fold change ≥2, $p \leq 0.05$) in hepatic macrophages from the two groups, of which 668 were upregulated and 203 were downregulated in *Gpr35*$^{-/-}$ mice compared to WT mice (Fig. 4A). Unsupervised hierarchical clustering of gene expression profiles showed clear separation between hepatic macrophages from APAP-treated *Gpr35*$^{-/-}$ and WT mice (Fig. 4B). Gene ontology (GO) analysis of the upregulated genes revealed that many biological processes were associated with inflammation in hepatic macrophages from APAP-treated *Gpr35*$^{-/-}$ mice (Fig. 4C). Gene set enrichment analysis (GSEA) yielded similar results, wherein a multitude of inflammatory processes were positively enriched in hepatic macrophages from APAP-treated *Gpr35*$^{-/-}$ mice, including PI3 K-Akt, NF-κB, and MAPK signaling pathways (Fig. 4D, E and F).

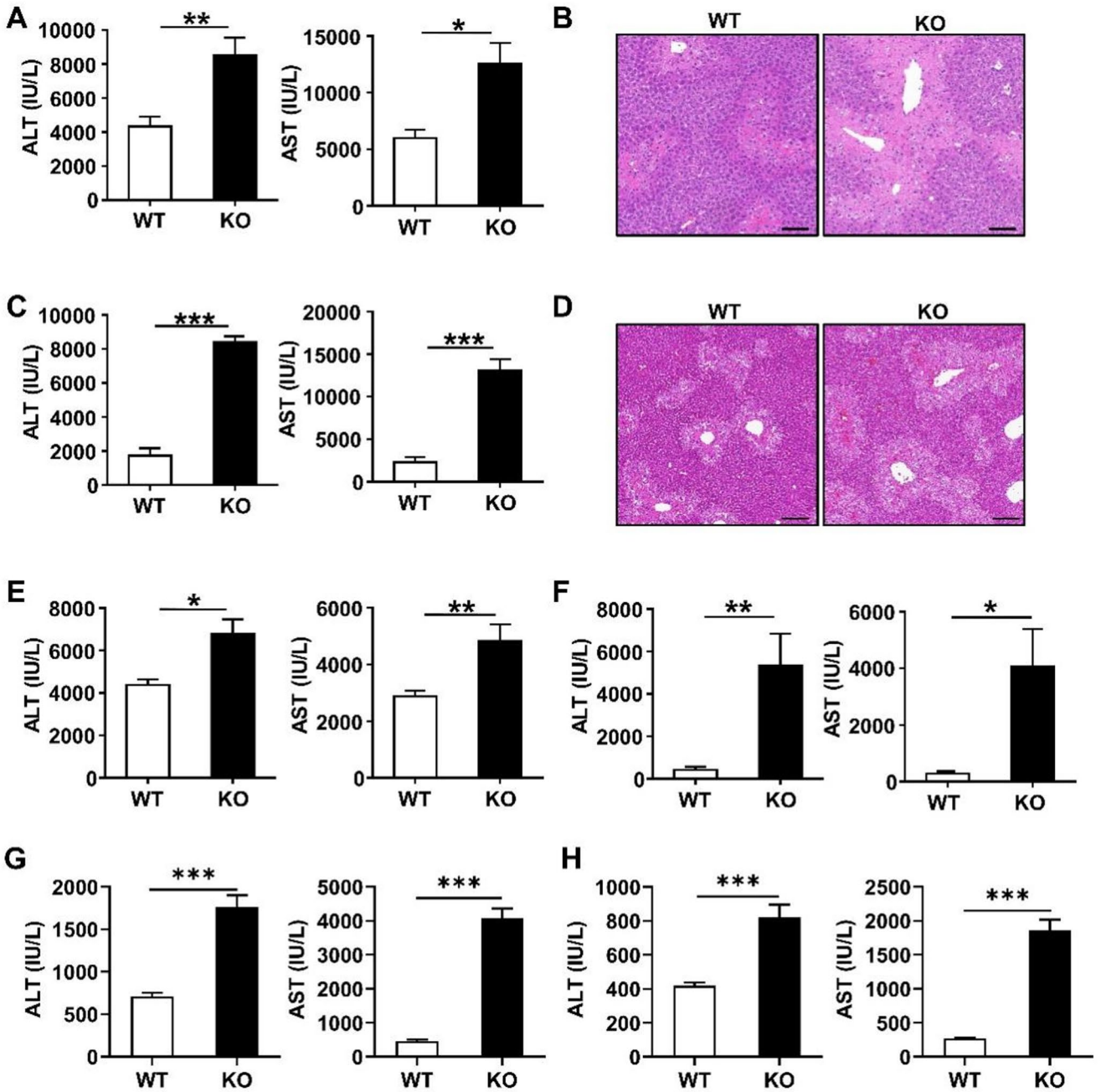

Fig. 1 GPR35 deficiency aggravates APAP-induced liver injury. (**A**) Levels of ALT and AST in sera from male WT mice and *Gpr35*$^{-/-}$ mice at 12 h after 400 mg/kg APAP challenge ($n = 5$). (**B**) Tissue damage in livers of male WT and *Gpr35*$^{-/-}$ mice at 12 h after 400 mg/kg APAP challenge, shown by hematoxylin and eosin staining (original magnification: ×20; scale bar: 100 μm). (**C**) Levels of ALT and AST in sera from female WT mice and *Gpr35*$^{-/-}$ mice at 12 h after 400 mg/kg APAP challenge ($n = 5$). (**D**) Tissue damage in livers of female WT and *Gpr35*$^{-/-}$ mice at 12 h after 400 mg/kg APAP challenge, shown by hematoxylin and eosin staining (original magnification: ×200; scale bar: 100 μm). (**E**) Levels of ALT and AST in sera from male WT mice and *Gpr35*$^{-/-}$ mice at 24 h after 300 mg/kg APAP challenge. (F) Levels of ALT and AST in sera from female WT mice and *Gpr35*$^{-/-}$ mice at 24 h after 300 mg/kg APAP challenge. (**G**) Levels of ALT and AST in sera from female WT mice and *Gpr35*$^{-/-}$ mice at 48 h after 300 mg/kg APAP challenge. (**H**) Levels of ALT and AST in sera from female WT mice and *Gpr35*$^{-/-}$ mice at 72 h after 300 mg/kg APAP challenge. The data are representative of three independent experiments and shown as the mean ± SEM. *, $P < 0.05$; **, $P < 0.01$; ***, $P < 0.001$

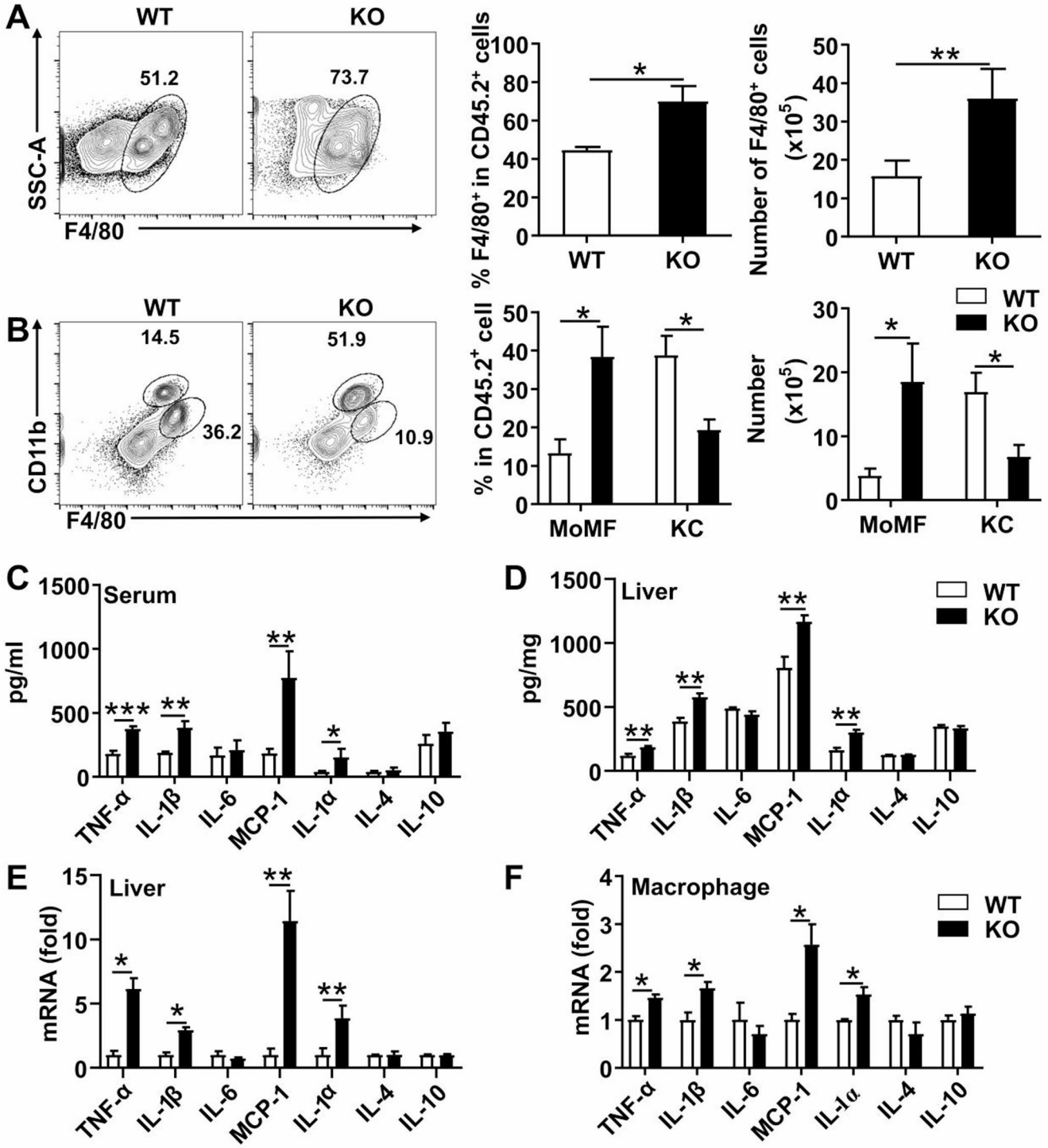

Fig. 2 GPR35 deficiency aggravates APAP-induced liver inflammation. (**A**) Frequency of total F4/80$^+$ cells in CD45$^+$ cells from livers of WT mice and *Gpr35*$^{-/-}$ mice treated with APAP. (**B**) Frequencies of MoMFs and KCs in CD45$^+$ cells from livers of WT mice and *Gpr35*$^{-/-}$ mice treated with APAP. (**C**) Levels of macrophage-associated cytokines in sera from WT mice and *Gpr35*$^{-/-}$ mice treated with APAP. (**D**) Protein levels of macrophage-associated cytokines in livers of WT mice and *Gpr35*$^{-/-}$ mice treated with APAP. (**E**) RNA levels of macrophage-associated cytokines in livers of WT mice and *Gpr35*$^{-/-}$ mice treated with APAP. (**F**) RNA levels of macrophage-associated cytokines in hepatic F4/80$^+$ cells from WT mice and *Gpr35*$^{-/-}$ mice treated with APAP. The data are representative of three independent experiments and shown as the mean ± SEM. *, $P < 0.05$; **, $P < 0.01$; ***, $P < 0.001$

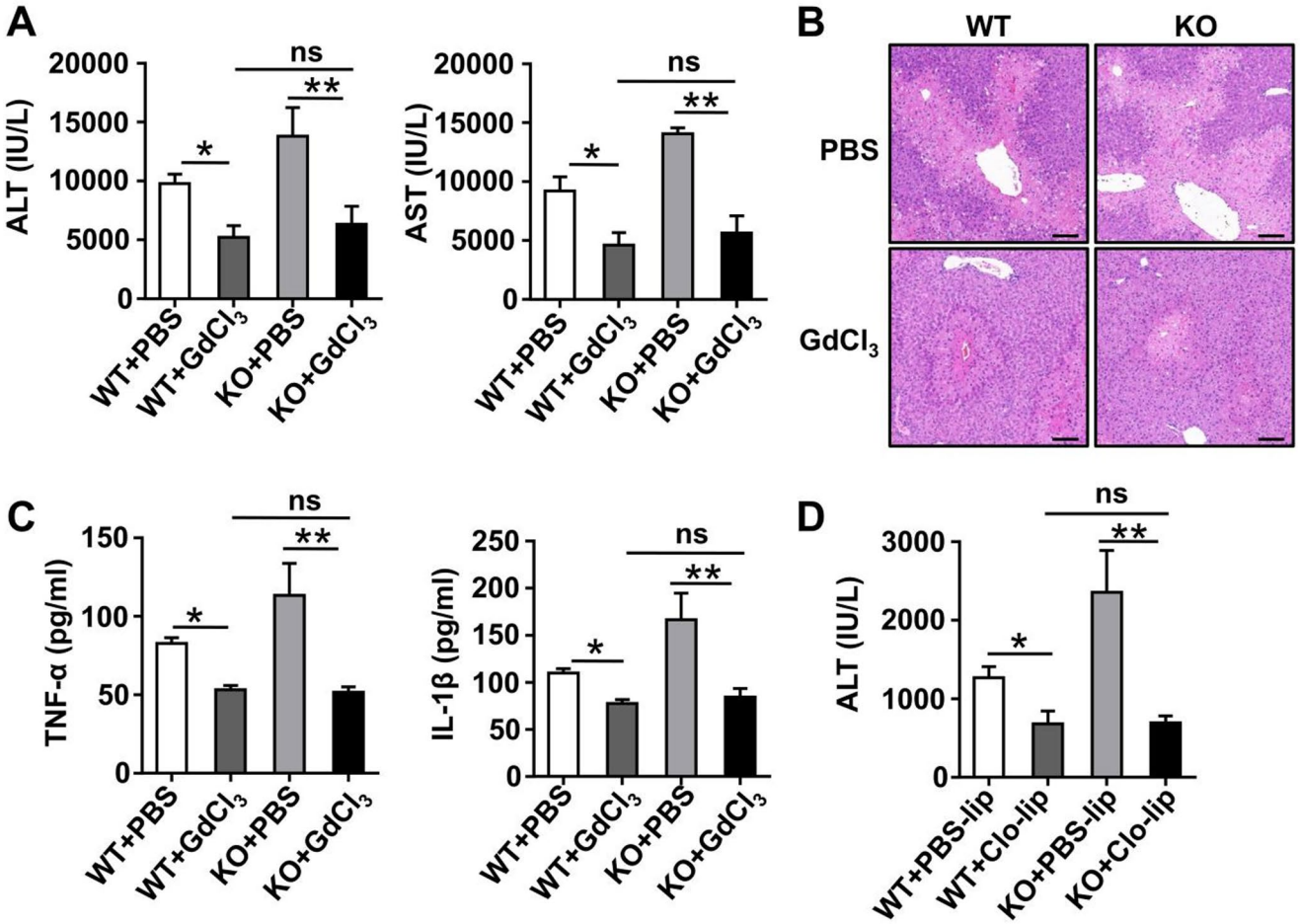

Fig. 3 Macrophage depletion abolishes the aggravation of liver injury induced by GPR35 deficiency. (**A**) Levels of ALT and AST in sera at 12 h after APAP challenge from WT mice and *Gpr35*$^{-/-}$ mice pretreated with PBS or $GdCl_3$. (**B**) Tissue damage in livers at 12 h after APAP challenge from WT mice and *Gpr35*$^{-/-}$ mice pretreated with PBS or $GdCl_3$, shown by hematoxylin and eosin staining (original magnification: ×20; scale bar: 100 μm). (**C**) Levels of TNF-α and IL-1β in sera at 12 h after APAP challenge from WT mice and *Gpr35*$^{-/-}$ mice pretreated with PBS or $GdCl_3$. (**D**) Levels of ALT in sera at 12 h after APAP challenge from WT mice and *Gpr35*$^{-/-}$ mice pretreated with PBS/liposome or clodronate/liposome. The data are representative of three independent experiments and shown as the mean ± SEM. *, $P < 0.05$; **, $P < 0.01$; ***, $P < 0.001$

These data suggest that GPR35 suppresses inflammatory signaling in macrophages.

Given the transcriptional differences in inflammatory processes between hepatic macrophages from APAP-treated *Gpr35*$^{-/-}$ and WT mice, we characterized their differences at the protein level using Western blot analysis. In agreement with the RNA-seq data, the levels of p-AKT, p-p38 and p-p65 were significantly elevated in macrophages obtained from *Gpr35*$^{-/-}$ mice (Fig. 5A). In contrast, pretreatment with the GPR35 agonist KA or DSCG prior to the APAP administration efficiently reduced inflammatory signaling, as evidenced by lower levels of p-AKT, p-p38, and p-p65 in macrophages from agonist-treated WT mice. These results suggested that GPR35 blocks the activation of inflammatory signaling in hepatic macrophages after APAP challenge (Fig. 5B). To further confirm these findings, peritoneal macrophages obtained from WT mice were stimulated with LPS in the presence of GPR35 agonists ex vivo. Treatment with GPR35 agonists attenuated the inflammatory response, characterized by decreased levels of p-AKT, p-p38, and p-p65 (Fig. 5C). Moreover, GPR35 agonists reduced pro-inflammatory cytokines in the supernatant, and decreased mRNA levels of pro-inflammatory cytokines in macrophages (Fig. 5D and E). Taken together, our findings demonstrate that GPR35 diminishes the inflammatory response in macrophages by dampening inflammatory signaling.

GPR35 dampens inflammatory signaling via the Gαs-cAMP-PKA pathway

To elucidate the downstream signaling by which GPR35 suppresses the inflammatory response in hepatic macrophages, the Co-IP assay of GPR35 was performed. GPR35 was identified to couple with Gαs (Fig. 6A). Gαs has been

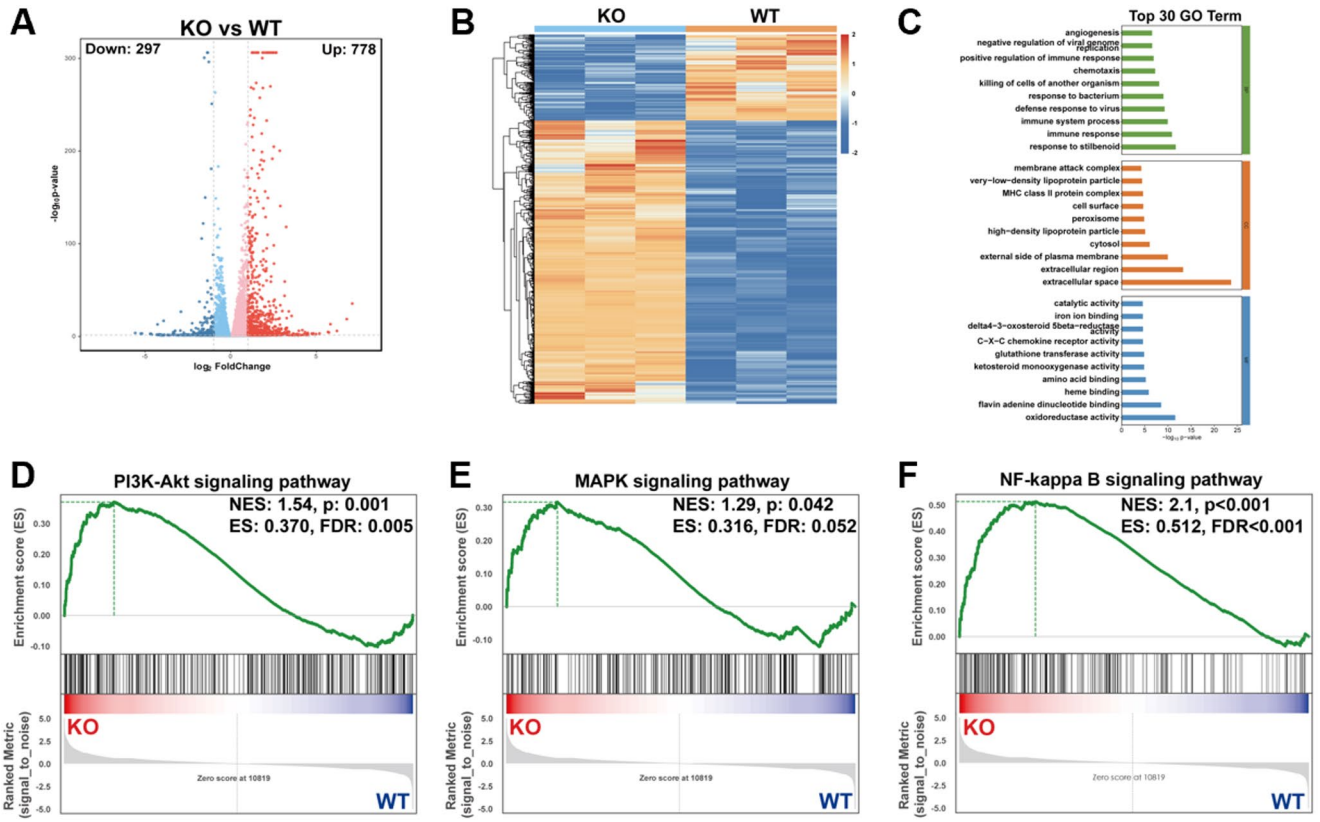

Fig. 4 GPR35 deficiency induces the inflammatory transcriptional feature in macrophages. (**A**) Volcano plot depicting DEGs in F4/80$^+$ hepatic macrophages from APAP-treated *Gpr35*$^{-/-}$ and WT mice. (**B**) RNA expression heatmap of DEGs in F4/80$^+$ hepatic macrophages from APAP-treated *Gpr35*$^{-/-}$ and WT mice. (**C**) GO enrichment of the top 30 enriched pathways for DEGs in F4/80$^+$ hepatic macrophages from APAP-treated *Gpr35*$^{-/-}$ and WT mice. (**D**-**F**) GSEA analysis between F4/80$^+$ hepatic macrophages from APAP-treated *Gpr35*$^{-/-}$ and WT mice using gene sets of (**D**) PI3 K-Akt signaling pathway, (**E**) MAPK signaling pathway, (**F**) NF-κB signaling pathway

reported to bind adenylyl cyclase (AC) and subsequently generate the second messenger cAMP [27]. The Gαs-cAMP signaling axis subsequently activates protein kinase A (PKA), specifically its catalytic subunit (PKA-C) [27]. Consistently, we observed an increase in the phosphorylation of the PKA catalytic subunit (p-PKA-C) (Supporting Fig. 4A). It has been reported that GPR35 can regulate intracellular signaling pathways through coupling with G12/13 [28]. Although the Co-IP assay identified an interaction between GPR35 and G12/13 proteins, our findings indicate that KA exerts its anti-inflammatory effects through GPR35 independently of G12/13 signaling. (Supporting Fig. 4B and C). Indeed, GPR35 agonists KA and DSCG and AC activator FSK elicited the intracellular production of cAMP in peritoneal macrophages (Fig. 6B). Likewise, GPR35 agonists KA and DSCG and AC activator FSK could suppressed the inflammatory response in macrophages ex vivo, as demonstrated by the decrease in pro-inflammatory cytokines in the presence of FSK (Fig. 6C). These findings indicated that the Gαs-cAMP-PKA pathway might be involved in GPR35-mediated suppression of the inflammatory response. To confirm this hypothesis, PKA inhibitor H89, AC inhibitor SQ22536, and Gαs inhibitor NF449 were added to LPS-stimulated macrophages before treatment with KA or DSCG. Of note, these inhibitors diminished the GPR35-mediated suppression of the inflammatory response in macrophages, as indicated by the increase in pro-inflammatory cytokines in the presence of Gαs-cAMP-PKA pathway inhibitors (Fig. 6D and E and Supporting Fig. 4D). These results indicate that GPR35 mitigates inflammatory signaling through the Gαs-cAMP-PKA pathway.

GPR35 agonists protect against APAP-induced liver injury

Next, we investigated whether GPR35 agonists could protect against APAP-induced liver injury. KA and DSCG were administered in vivo to mice treated with APAP, and both agonists effectively mitigated liver injury, as evidenced by reduced serum ALT and AST levels and decreased liver damage (Fig. 7A, B, D and E). Meanwhile, the levels of pro-inflammatory cytokines in the sera were significantly reduced (Fig. 7C and F). Additionally, other GPR35 agonists 5-HIAA and Zaprinast also inhibited LPS-induced

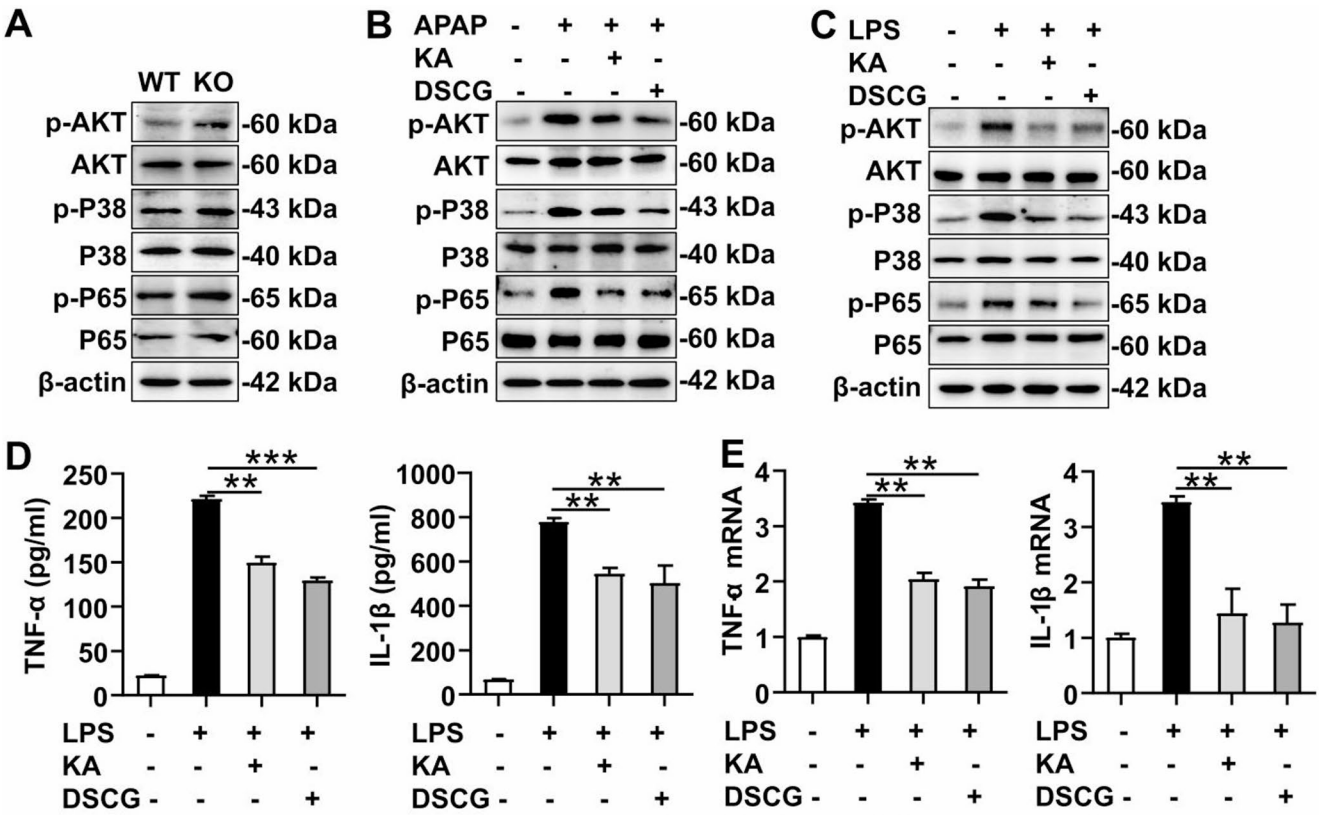

Fig. 5 GPR35 deficiency enhances the inflammatory response in macrophages. (**A**) Levels of inflammatory signaling molecules in hepatic F4/80^{+} cells from WT mice and *Gpr35*$^{-/-}$ mice at 12 h after APAP challenge. (**B**) Levels of inflammatory signaling molecules in hepatic F4/80^{+} cells from WT mice pretreated with KA or DSCG at 12 h after APAP challenge. (**C**) Levels of inflammatory signaling molecules in peritoneal macrophages from WT mice at 12 h after LPS stimulation with or without KA or DSCG. (**D**) Levels of TNF-α and IL-1β in supernatants from peritoneal macrophages of WT mice at 12 h after LPS stimulation ex vivo with or without KA or DSCG. (**E**) mRNA levels of TNF-α and IL-1β in peritoneal macrophages of WT mice at 12 h after LPS stimulation ex vivo with or without KA or DSCG. The data are representative of three independent experiments and shown as the mean ± SEM. *, $P < 0.05$; **, $P < 0.01$; ***, $P < 0.001$

TNF-α elevation. Moreover, KA demonstrated anti-inflammatory effects in human THP-1 cells (Supporting Fig. 5). Taken together, these findings further confirm that GPR35 activation protects against APAP-induced liver injury by suppressing the inflammatory response.

GPR35 agonists protect against LPS/D-GalN-induced liver injury

It has been confirmed that hepatic macrophage-mediated inflammation is a major contributor to LPS/D-GalN-induced acute liver injury. Therefore, we investigated whether GPR35 protects against LPS/D-GalN-induced liver injury. *Gpr35*$^{-/-}$ mice developed more severe liver injury than WT mice, as demonstrated by higher ALT and AST levels and larger damaged areas in *Gpr35*$^{-/-}$ mice (Fig. 8A and B). In addition, the levels of pro-inflammatory cytokines in the sera were markedly higher in *Gpr35*$^{-/-}$ mice (Fig. 8E), suggesting that GPR35 deficiency aggravates LPS/D-GalN-induced inflammation and liver injury. Of note, GPR35 agonists were capable of attenuating LPS/D-GalN-induced acute liver injury, which was marked by lower ALT and AST levels, reduced damaged areas, and decreased levels of pro-inflammatory cytokines (Fig. 8C, D and F). Collectively, our findings demonstrate that GPR35 protects against LPS/D-GalN-induced inflammation-mediated liver injury.

Discussion

This study revealed a protective role of GPR35 in drug-induced liver injury via the inhibition of macrophage-mediated inflammation. The absence of GPR35 aggravates drug-induced liver inflammation and damage. In contrast, GPR35 agonists effectively protect against drug-induced liver inflammation and damage (Fig. 9). This study provides novel insights into the role of GPR35 in drug-induced liver injury.

Genome-wide association studies have identified that the mutation of GPR35 is associated with increased risk of

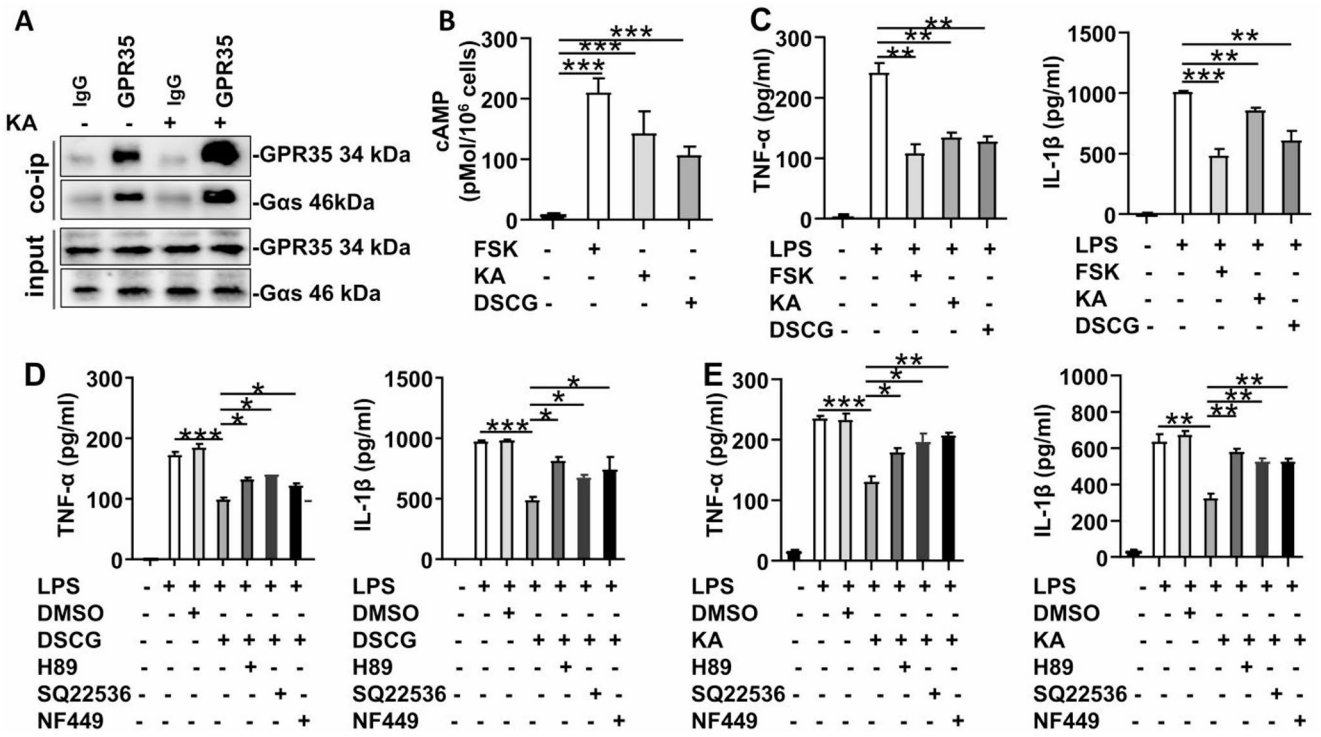

Fig. 6 GPR35 attenuates inflammatory response in macrophages through the Gαs-cAMP-PKA pathway. (**A**) Co-IP detection of GPR35 and Gαs in peritoneal macrophages stimulated with or without KA. (**B**) Levels of cAMP in peritoneal macrophages pretreated with FSK, KA, or DSCG. GPR35 agonist KA (4 mM), or DSCG (200 μg/ml) was administered 1 h before treatment with LPS. Adenylate cyclase activator FSK (10 μM) was used to stimulate cAMP in peritoneal macrophages 1 h before treatment with LPS. (**C**) Levels of TNF-α and IL-1β in supernatants from peritoneal macrophages after stimulation with LPS in the presence of FSK, KA, or DSCG. (**D**) Levels of TNF-α and IL-1β in supernatants from peritoneal macrophages with indicated pretreatment after LPS stimulation. (**E**) Levels of TNF-α and IL-1β in supernatants from peritoneal macrophages with indicated pretreatment after LPS stimulation. Gαs inhibitor NF449, AC inhibitor SQ22536, or PKA inhibitor H89 was added to the culture 30 min before treatment with GPR35 agonist KA or DSCG. The data are representative of three independent experiments and shown as the mean ± SEM. *, $P < 0.05$; **, $P < 0.01$; ***, $P < 0.001$

digestive system diseases, such as inflammatory bowel disease, primary sclerosing cholangitis, and autoimmune liver disease [29, 30]. The roles of GPR35 in inflammatory bowel disease have been extensively investigated [31–33]. Nonetheless, the roles of GPR35 in liver diseases remain unclear. GPR35 is expressed in Hep3B human hepatoma cells and mouse primary hepatocytes [34]. It has been reported that the putative agonist of GPR35 lodoxamide suppresses lipid accumulation, improves high fat diet-induced fatty liver, and attenuates CCl_4-induced liver fibrosis [34, 35]. However, results obtained from a TGF-α shedding assay showed that lodoxamide activates human GPR35, but not mouse GPR35, in vitro [35]. Meanwhile, GPR35 antagonist CID2745687 is species-specific and only effective in inhibiting human GPR35 [36]. These findings raise concerns regarding the dependence of lodoxamide action on GPR35 in mice. Thus, the roles of GPR35 in liver diseases warrant further investigation. We found that GPR35 alleviated APAP-induced liver injury. The similar levels of CYP2E1 and GSH, two key molecules regulating APAP metabolism and detoxication, in WT mice and *Gpr35*$^{-/-}$ mice, indicate that GPR35 did not be involved in the regulation of APAP metabolism/NAPQI-induced hepatotoxicity (Supporting Fig. 6). In addition, we found that GPR35 suppressed NLRP3 inflammasome activation in macrophages [23]. Therefore, these data drive us to investigate the role of macrophages in GPR35-mediated protection during APAP challenge.

Macrophages have been recognized as the central modulator of hepatic inflammation and resolution during APAP-induced liver injury. We previously found that macrophages generated multiple pro-inflammatory mediators to mediate the second-hit after APAP challenge [7]. Our findings revealed that GPR35 deficiency increased the production of pro-inflammatory cytokines by macrophages, whereas GPR35 agonists exerted an anti-inflammatory effect. Moreover, the GPR35-dependent protection disappeared after the depletion of macrophages. Thus, our findings identified the roles of GPR35 in regulating pro-inflammatory macrophages, indicating that it may be a useful target for the treatment of macrophage-mediated hepatic inflammation. Consistently, GPR35-dependent protection also dampened LPS/D-GalN-induced liver injury. Macrophages improve

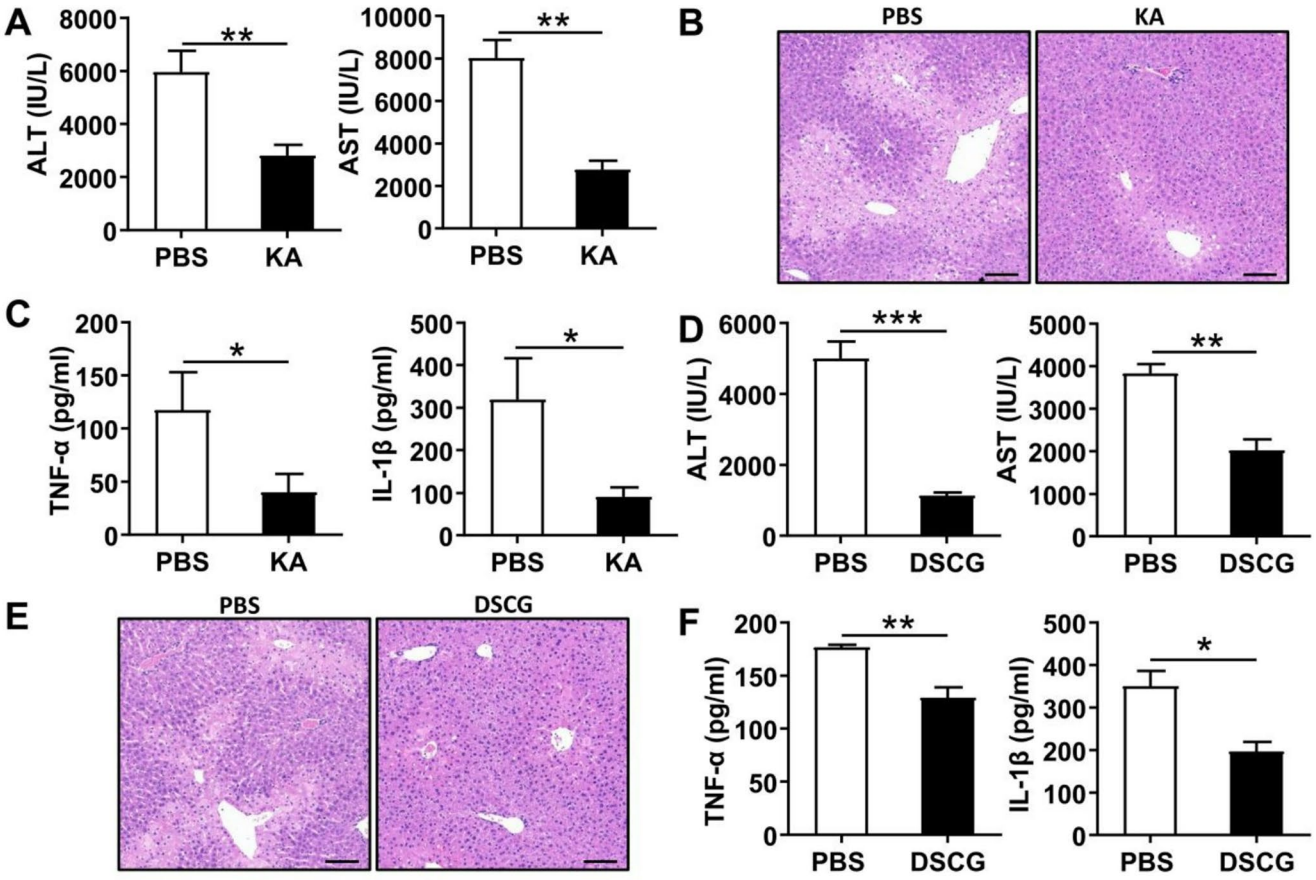

Fig. 7 GPR35 agonists alleviate APAP-induced liver injury. (**A**) Levels of ALT and AST in sera at 12 h after APAP challenge from WT mice pretreated with PBS or KA. (**B**) Tissue damage in livers at 12 h after APAP challenge from WT mice pretreated with PBS or KA, shown by hematoxylin and eosin staining (original magnification: ×20; scale bar: 100 μm). (**C**) Levels of TNF-α and IL-1β in sera at 12 h after APAP challenge from WT mice pretreated with PBS or KA. (**D**) Levels of ALT and AST in sera at 12 h after APAP challenge from WT mice pretreated with PBS or DSCG. (**E**) Tissue damage in livers at 12 h after APAP challenge from WT mice pretreated with PBS or DSCG, shown by hematoxylin and eosin staining (original magnification: ×200; scale bar: 100 μm). (**F**) Levels of TNF-α and IL-1β in sera at 12 h after APAP challenge from WT mice pretreated with PBS or DSCG. The data are representative of three independent experiments and shown as the mean ± SEM. *, $P < 0.05$; **, $P < 0.01$; ***, $P < 0.001$

the resolution of damage at the late stage after treatment with APAP. It has been shown that resolution-promoting Ly6 $C^{lo}CX3$ $CR1^{hi}$ macrophages improve liver repair during APAP-induced liver injury [37]. The adoptive transfer of these alternatively activated macrophages is able to promote the resolution of APAP-induced liver injury [38]. $MerTK^{+}$ hepatic macrophages has also been reported promote the resolution of inflammation following APAP-induced liver injury [39]. Therefore, it is necessary to further examine whether GPR35 promotes the transition of pro-inflammatory macrophages to resolution-promoting macrophages and the resolution of inflammation following APAP challenge.

GPR35 activation primes diverse downstream signaling pathways and modulates multiple cellular processes in a context- and species-dependent manner. Human or rat GPR35 has been found to activate Gi/o family G proteins [40]. In addition, it has been reported that, upon activation by agonists, GPR35 recruits β-arrestin-2 and activates Gα13 [41]. Also, it has been shown that mouse GPR35 interacts with and promotes the activity of Na/K-ATPase in macrophages [32]. In this study, we found that GPR35 interacted with Gαs, which activates ACs to catalyze the synthesis of cAMP from ATP, leading to an increase in intracellular cAMP. The inhibition of Gαs-cAMP-PKA signaling with specific inhibitors partially reversed the GPR35-mediated suppression of the inflammatory response. Our findings implied the interaction of GPR35 with Gαs mediates the anti-inflammatory effect in macrophages. NF449 served as an agent to inhibit Gαs, future studies will require the development of more selective, cell-permeable Gαs inhibitors to more accurately confirm these findings. Additionally, the identification of other downstream signals of GPR35 that may be involved in the GPR35-mediated suppression of the inflammatory response need further investigations.

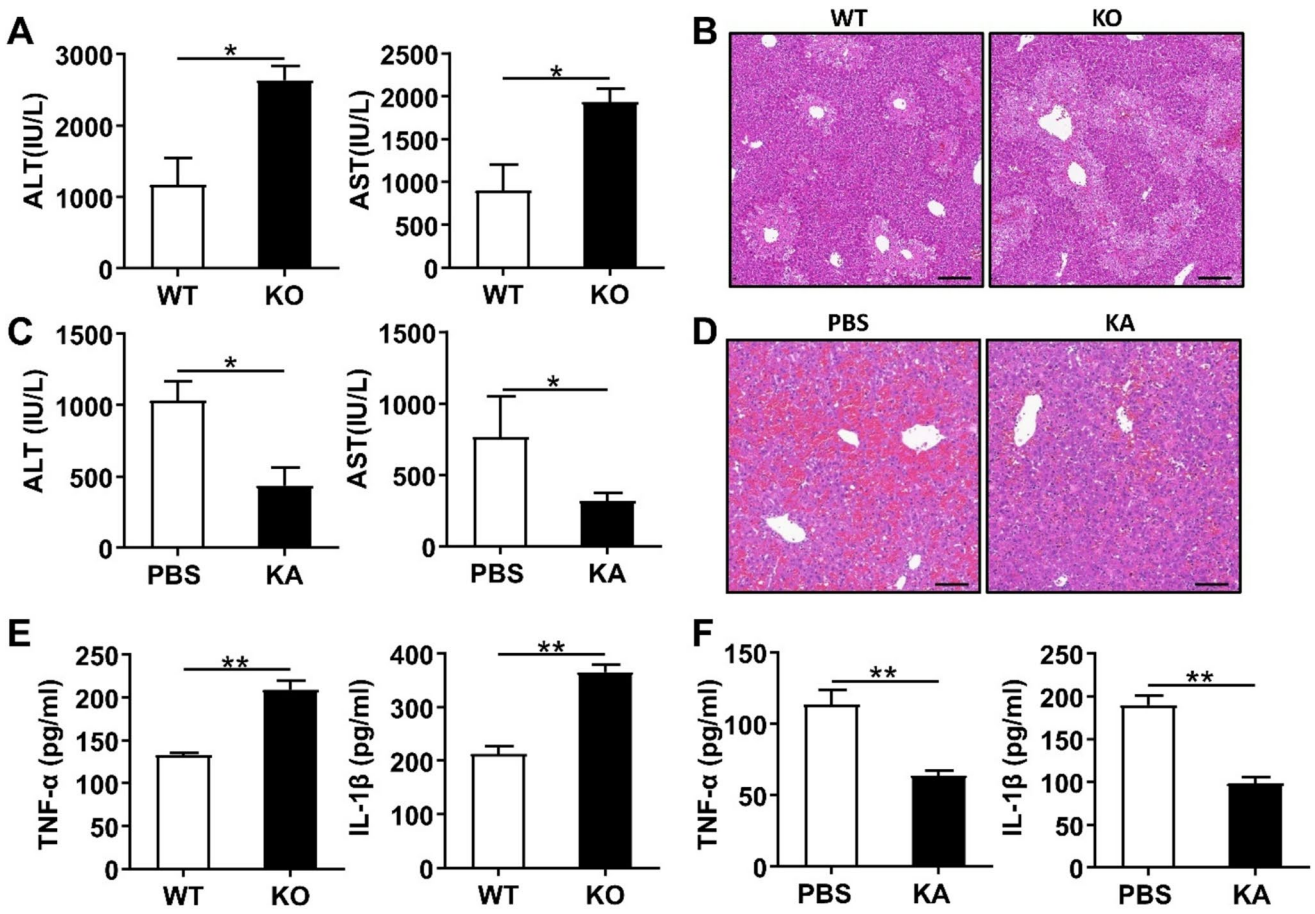

Fig. 8 The GPR35 agonist alleviates LPS/D-GalN-induced liver injury. (**A**) Levels of ALT and AST in sera from WT mice and *Gpr35*$^{-/-}$ mice at 12 h after LPS/D-GalN challenge ($n = 5$). (**B**) Tissue damage in livers of male WT and *Gpr35*$^{-/-}$ mice at 12 h after LPS/D-GalN challenge, shown by hematoxylin and eosin staining (original magnification: ×20; scale bar: 100 μm). (**C**) Levels of ALT and AST in sera at 12 h after LPS challenge from WT mice pretreated with PBS or KA. (**D**) Tissue damage in livers at 12 h after LPS challenge from WT mice pretreated with PBS or KA, shown by hematoxylin and eosin staining (original magnification: ×200; scale bar: 100 μm). (**E**) Levels of TNF-α and IL-1β in sera from WT mice and *Gpr35*$^{-/-}$ mice at 12 h after LPS challenge. (**F**) Levels of TNF-α and IL-1β in sera at 12 h after LPS challenge from WT mice pretreated with PBS or KA. The data are representative of three independent experiments and shown as the mean ± SEM. *, $P < 0.05$; **, $P < 0.01$; ***, $P < 0.001$

KA is the putative ligand of GPR35 and found in high levels in bile, pancreatic juice, and the intestine excretion [40, 42]. Nonetheless, the low affinity of KA for human GPR35 questions its role as the real endogenous ligand for GPR35 [43]. Therefore, it is necessary to identify other effective ligands of GPR35 in vivo. C-X-C motif chemokine ligand 17 (CXCL17), LPA, and 5-HIAA have also been suggested as putative ligands of GPR35 [15, 16, 44]. Moreover, synthetic agonists and antagonists have been developed to regulate GPR35 activity. However, accumulating studies suggest that these ligands modulate GPR35 in a species- and context-dependent manner [45]. As evidence supports GPR35 as a valuable therapeutic target for various diseases, such as inflammatory bowel disease and hypertension, more efforts are needed to develop GPR35-specific agonists and antagonists [46].

In summary, the present data revealed that GPR35 alleviates APAP-induced liver injury via the Gαs-cAMP-PKA pathway. Moreover, GPR35 agonists could suppress macrophage-mediated inflammation and improve drug-induced live injury. Our findings indicate that GPR35 may serve as a target for the development of novel medicines that control drug-induced liver injury.

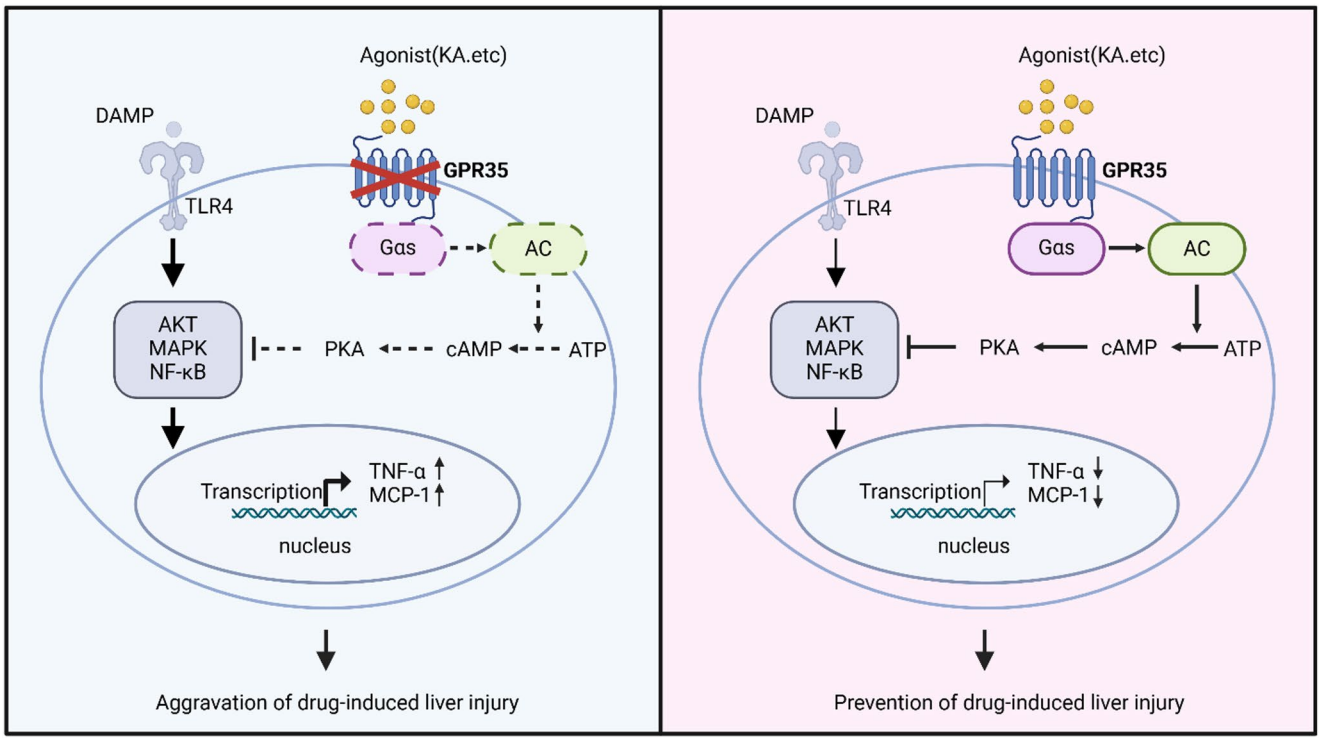

Fig. 9 Working models of GPR35-mediated protection in APAP-induced liver injury. GPR35 prevents drug-induced liver injury by blocking macrophage-mediated inflammation via the Gαs-cyclic AMP-protein kinase A pathway

Supplementary Information The online version contains supplementary material available at https://doi.org/10.1007/s00018-025-05751-4.

Author contributions XQZ, YHL, LY designed and conducted experiments, analyzed and interpreted data. XC JLZ, TC, CYX, FL, HQW conducted some experiments, JJW, JJC reviewed and revised the manuscript. XFW, JL, WWY conceptualized and supervised the study, designed experiments and wrote the manuscript.

Funding This study is supported by the National Natural Science Foundation of China (grant numbers 82070608, 8220033805 and 82371756), the Science Fund of Universities of Anhui Province for Distinguished Young Scholars (2023 AH020032), Anhui Provincial Natural Science Foundation (grant number 2108085Y28 and 2208085Y26), the Supporting Program for Outstanding Young Talents in Universities of Anhui Province of China (gxyqZD2021103), the Promotion Plan of Basic and Clinical Cooperative Research in Anhui Medical University (2021xkjT035).

Data availability Supporting data for this manuscript are available in the Supplementary Material and all other data are available upon request.

Declarations

Ethical approval The animal study conducted in this manuscript was conducted according to the approved animal ethics protocol LLSC20200725 approved by the Local Ethics Committee for Animal Care and Use at Anhui Medical University.

Consent for publication All authors commented on previous versions of the manuscript and approved the final manuscript. All authors have consented for publication of this manuscript.

Conflict of interest The authors have no relevant financial or non-financial interests to disclose.

References

1. Chowdhury A, Nabila J, Adelusi Temitope I, Wang S (2020) Current etiological comprehension and therapeutic targets of acetaminophen-induced hepatotoxicity. Pharmacol Res 161:105102
2. Yan M, Huo Y, Yin S, Hu H (2018) Mechanisms of acetaminophen-induced liver injury and its implications for therapeutic interventions. Redox Biol 17:274–283
3. Andrade RJ, Chalasani N, Bjornsson ES, Suzuki A, Kullak-Ublick GA, Watkins PB, Devarbhavi H et al (2019) Drug-induced liver injury. Nat Rev Dis Primers 5:58

4. Hendrickson RG (2019) What is the most appropriate dose of N-acetylcysteine after massive acetaminophen overdose? Clin Toxicol (Phila) 57:686–691
5. Rushworth GF, Megson IL (2014) Existing and potential therapeutic uses for N-acetylcysteine: the need for conversion to intracellular glutathione for antioxidant benefits. Pharmacol Ther 141:150–159
6. Wang X, Sun R, Chen Y, Lian ZX, Wei H, Tian Z (2015) Regulatory T cells ameliorate acetaminophen-induced immune-mediated liver injury. Int Immunopharmacol 25:293–301
7. Wang X, Sun R, Wei H, Tian Z (2013) High-mobility group box 1 (HMGB1)-Toll-like receptor (TLR)4-interleukin (IL)-23-IL-17A axis in drug-induced damage-associated lethal hepatitis: interaction of gammadelta T cells with macrophages. Hepatology 57:373–384
8. Mossanen JC, Krenkel O, Ergen C, Govaere O, Liepelt A, Puengel T, Heymann F et al (2016) Chemokine (C-C motif) receptor 2-positive monocytes aggravate the early phase of acetaminophen-induced acute liver injury. Hepatology 64:1667–1682
9. Clemens MM, Vazquez JH, Kennon-McGill S, McCullough SS, James LP, McGill MR (2020) Pre-treatment twice with liposomal clodronate protects against acetaminophen hepatotoxicity through a pre-conditioning effect. Liver Res 4:145–152
10. Biagioli M, Carino A, Fiorucci C, Marchiano S, Di Giorgio C, Bordoni M, Roselli R et al (2020) The bile acid receptor GPBAR1 modulates CCL2/CCR2 signaling at the liver sinusoidal/macrophage interface and reverses Acetaminophen-Induced liver toxicity. J Immunol 204:2535–2551
11. Antoniades CG, Khamri W, Abeles RD, Taams LS, Triantafyllou E, Possamai LA, Bernsmeier C et al (2014) Secretory leukocyte protease inhibitor: a pivotal mediator of anti-inflammatory responses in acetaminophen-induced acute liver failure. Hepatology 59:1564–1576
12. Congreve M, de Graaf C, Swain NA, Tate CG (2020) Impact of GPCR structures on drug discovery. Cell 181:81–91
13. Wootten D, Christopoulos A, Marti-Solano M, Babu MM, Sexton PM (2018) Mechanisms of signalling and biased agonism in G protein-coupled receptors. Nat Rev Mol Cell Biol 19:638–653
14. Quon T, Lin LC, Ganguly A, Tobin AB, Milligan G (2020) Therapeutic opportunities and challenges in targeting the orphan G Protein-Coupled receptor GPR35. ACS Pharmacol Transl Sci 3:801–812
15. De Giovanni M, Tam H, Valet C, Xu Y, Looney MR, Cyster JG (2022) GPR35 promotes neutrophil recruitment in response to serotonin metabolite 5-HIAA. Cell 185:815–830e819
16. Kaya B, Donas C, Wuggenig P, Diaz OE, Morales RA, Melhem H, Swiss IBDCI et al (2020) Lysophosphatidic Acid-Mediated GPR35 signaling in CX3CR1(+) macrophages regulates intestinal homeostasis. Cell Rep 32:107979
17. Agudelo LZ, Ferreira DMS, Cervenka I, Bryzgalova G, Dadvar S, Jannig PR, Pettersson-Klein AT et al (2018) Kynurenic acid and Gpr35 regulate adipose tissue energy homeostasis and inflammation. Cell Metab 27:378–392e375
18. De Giovanni M, Dang EV, Chen KY, An J, Madhani HD, Cyster JG (2023) Platelets and mast cells promote pathogenic eosinophil recruitment during invasive fungal infection via the 5-HIAA-GPR35 ligand-receptor system. Immunity 56:1548–1560e1545
19. Kim C, Kim Y, Lim JY, Kim M, Zheng H, Kim M, Hwang SW (2023) Pamoic acid-induced peripheral GPR35 activation improves pruritus and dermatitis. Br J Pharmacol 180:3059–3070
20. Cheng L, Wu H, Cai X, Zhang Y, Yu S, Hou Y, Yin Z et al (2024) A Gpr35-tuned gut microbe-brain metabolic axis regulates depressive-like behavior. Cell Host Microbe 32:227–243e226
21. Milligan G (2023) GPR35: from enigma to therapeutic target. Trends Pharmacol Sci 44:263–273
22. Wyant GA, Yu W, Doulamis IP, Nomoto RS, Saeed MY, Duignan T, McCully JD et al (2022) Mitochondrial remodeling and ischemic protection by G protein-coupled receptor 35 agonists. Science 377:621–629
23. Sun T, Xie R, He H, Xie Q, Zhao X, Kang G, Cheng C et al (2022) Kynurenic acid ameliorates NLRP3 inflammasome activation by blocking calcium mobilization via GPR35. Front Immunol 13:1019365
24. Wei X, Yin F, Wu M, Xie Q, Zhao X, Zhu C, Xie R et al (2023) G protein-coupled receptor 35 attenuates nonalcoholic steatohepatitis by reprogramming cholesterol homeostasis in hepatocytes. Acta Pharm Sin B 13:1128–1144
25. Xu F, Guo M, Huang W, Feng L, Zhu J, Luo K, Gao J et al (2020) Annexin A5 regulates hepatic macrophage polarization via directly targeting PKM2 and ameliorates NASH. Redox Biol 36:101634
26. Zhang X, Goncalves R, Mosser DM (2008) The isolation and characterization of murine macrophages. Curr Protoc Immunol Chap. 14:Unit 14 11
27. Rayees S, Joshi JC, Tauseef M, Anwar M, Baweja S, Rochford I, Joshi B et al (2019) PAR2-Mediated cAMP generation suppresses TRPV4-Dependent Ca(2+) signaling in alveolar macrophages to resolve TLR4-Induced inflammation. Cell Rep 27:793–805e794
28. Fallarini S, Magliulo L, Paoletti T, de Lalla C, Lombardi G (2010) Expression of functional GPR35 in human iNKT cells. Biochem Biophys Res Commun 398:420–425
29. Ellinghaus D, Folseraas T, Holm K, Ellinghaus E, Melum E, Balschun T, Laerdahl JK et al (2013) Genome-wide association analysis in primary sclerosing cholangitis and ulcerative colitis identifies risk loci at GPR35 and TCF4. Hepatology 58:1074–1083
30. Li X, Shen J, Ran Z (2017) Crosstalk between the gut and the liver via susceptibility loci: novel advances in inflammatory bowel disease and autoimmune liver disease. Clin Immunol 175:115–123
31. Farooq SM, Hou Y, Li H, O'Meara M, Wang Y, Li C, Wang JM (2018) Disruption of GPR35 exacerbates dextran sulfate Sodium-Induced colitis in mice. Dig Dis Sci 63:2910–2922
32. Schneditz G, Elias JE, Pagano E, Zaeem Cader M, Saveljeva S, Long K, Mukhopadhyay S et al (2019) GPR35 promotes glycolysis, proliferation, and oncogenic signaling by engaging with the sodium potassium pump. Sci Signal 12(562):eaau9048
33. Tsukahara T, Hamouda N, Utsumi D, Matsumoto K, Amagase K, Kato S (2017) G protein-coupled receptor 35 contributes to mucosal repair in mice via migration of colonic epithelial cells. Pharmacol Res 123:27–39
34. Nam SY, Park SJ, Im DS (2019) Protective effect of lodoxamide on hepatic steatosis through GPR35. Cell Signal 53:190–200
35. Kim MJ, Park SJ, Nam SY, Im DS (2019) Lodoxamide attenuates hepatic fibrosis in mice: involvement of GPR35. Biomol Ther (Seoul) 28(1):92–97
36. Jenkins L, Harries N, Lappin JE, MacKenzie AE, Neetoo-Isseljee Z, Southern C, McIver EG et al (2012) Antagonists of GPR35 display high species ortholog selectivity and varying modes of action. J Pharmacol Exp Ther 343:683–695
37. Yang W, Tao Y, Wu Y, Zhao X, Ye W, Zhao D, Fu L et al (2019) Neutrophils promote the development of reparative macrophages mediated by ROS to orchestrate liver repair. Nat Commun 10:1076
38. Starkey Lewis P, Campana L, Aleksieva N, Cartwright JA, Mackinnon A, O'Duibhir E, Kendall T et al (2020) Alternatively activated macrophages promote resolution of necrosis following acute liver injury. J Hepatol 73:349–360
39. Triantafyllou E, Pop OT, Possamai LA, Wilhelm A, Liaskou E, Singanayagam A, Bernsmeier C et al (2018) MerTK expressing hepatic macrophages promote the resolution of inflammation in acute liver failure. Gut 67:333–347

40. Wang J, Simonavicius N, Wu X, Swaminath G, Reagan J, Tian H, Ling L (2006) Kynurenic acid as a ligand for orphan G protein-coupled receptor GPR35. J Biol Chem 281:22021–22028
41. Jenkins L, Brea J, Smith NJ, Hudson BD, Reilly G, Bryant NJ, Castro M et al (2010) Identification of novel species-selective agonists of the G-protein-coupled receptor GPR35 that promote recruitment of beta-arrestin-2 and activate Galpha13. Biochem J 432:451–459
42. Paluszkiewicz P, Zgrajka W, Saran T, Schabowski J, Piedra JL, Fedkiv O, Rengman S et al (2009) High concentration of kynurenic acid in bile and pancreatic juice. Amino Acids 37:637–641
43. Jenkins L, Alvarez-Curto E, Campbell K, de Munnik S, Canals M, Schlyer S, Milligan G (2011) Agonist activation of the G protein-coupled receptor GPR35 involves transmembrane domain III and is transduced via Galpha(1)(3) and beta-arrestin-2. Br J Pharmacol 162:733–748
44. Maravillas-Montero JL, Burkhardt AM, Hevezi PA, Carnevale CD, Smit MJ, Zlotnik A (2015) Cutting edge: GPR35/CXCR8 is the receptor of the mucosal chemokine CXCL17. J Immunol 194:29–33
45. Binti Mohd Amir NAS, Mackenzie AE, Jenkins L, Boustani K, Hillier MC, Tsuchiya T, Milligan G et al (2018) Evidence for the existence of a CXCL17 receptor distinct from GPR35. J Immunol 201:714–724
46. Wu Y, Zhang P, Fan H, Zhang C, Yu P, Liang X, Chen Y (2023) GPR35 acts a dual role and therapeutic target in inflammation. Front Immunol 14:1254446